Improvement of the accuracy of liver lesion DCEUS quantification with the use of automatic respiratory gating

Damianos Christofides[1] · Edward L. S. Leen[2] · Michalakis A. Averkiou[1]

Abstract

Objectives To evaluate the efficiency of automatic respiratory gating (ARG) in reducing respiratory motion-induced artefacts from dynamic contrast-enhanced ultrasound (DCEUS) acquisitions and to assess the impact of ARG on DCEUS quantification parameters in patients with liver malignancies.

Methods Twenty-five patients with liver metastasis were imaged with DCEUS. The lognormal indicator dilution model was fitted on time-intensity curves extracted from hepatic lesions with and without the use of ARG and DCEUS quantification parameters were extracted. The goodness of fit was assessed using the coefficient of determination (R^2_{LN}). The effect respiration had on the data was assessed using the respiration amplitude (RA) metric. Pearson's correlation coefficient (r) was used to assess the correlation between R^2_{LN} and RA with and without the use of ARG.

Results The RA parameter was strongly correlated with R^2_{LN} ($r=-0.96$, $P=7.412\times10^{-15}$) and this correlation became weaker with ARG ($r=-0.64$, $P=5.449\times10^{-4}$). ARG significantly influenced the values of the quantification parameters extracted ($P\leq0.05$). The RA was significantly decreased when ARG was used ($P=1.172\times10^{-6}$).

Conclusions ARG has a significant impact on the quantification parameters extracted and it has been shown to improve the accuracy of liver lesion DCEUS.

✉ Michalakis A. Averkiou
  maverk@ucy.ac.cy

1 Department of Mechanical and Manufacturing Engineering, University of Cyprus, 75 Kallipoleos Street, 1678 Nicosia, Cyprus

2 Department of Experimental Medicine, Imperial College London, Hammersmith Hospital, Du Cane Road, London W12 0HS, England

Key Points
- *ARG has a significant impact on DCEUS quantification parameters.*
- *ARG can improve the modelling of liver lesion haemodynamics using DCEUS quantification.*
- *ARG significantly reduces the respiration amplitude of DCEUS lesion time-intensity curves.*

Introduction

Studies have shown that dynamic contrast-enhanced ultrasound (DCEUS) can be used for early evaluation of response to anti-angiogenic treatment of patients with liver and renal cancers [1–4]. Indicator dilution theory can be used to model lesion haemodynamics and extract blood flow parameters [5]. The DCEUS quantification parameters relating to lesion perfusion may provide for an early detection of patient response to treatment [6, 7]. Various factors can affect the image intensity in DCEUS loops such as signal saturation, acoustic shadowing, nonlinear propagation of ultrasound, beam non-uniformity, ultrasound probe motion and system settings [8–10].

Respiratory motion is a major limitation in the accurate measurement of the time-intensity curve parameters, especially in liver imaging by introducing noise in the curves. Typically, a region-of-interest (ROI) is drawn around the lesion and the average pixel intensity is measured as a function of time forming the time-intensity curve of the lesion. Respiration causes the lesion to move in and out of the ROI, thus the image intensity within the ROI may also have components arising from sampling of normal tissue and/or vessels (Fig. 1) that shows as added noise in the data (Fig. 3a).
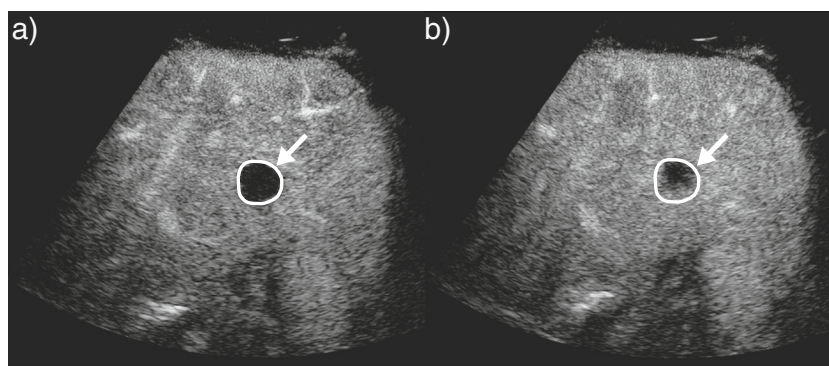
Fig. 1 Demonstration of a lesion moving (**a**) inside and (**b**) outside a region-of-interest (ROI) (indicated by the arrow) at two different time points of the DCEUS acquisition. In (**a**) the mean intensity value within the ROI is representative of the lesion perfusion whereas in (**b**) the ROI also includes part of the liver parenchyma, and thus the mean linear intensity value extracted is not representative of lesion perfusion

Respiratory gating algorithms have been suggested in the literature as a possible solution to limiting the effect of breathing motion [11–14]. Here we evaluated an algorithm for automatic respiratory gating (ARG) in a clinical study for efficiency in reducing the effect of respiratory motion from DCEUS loops [15]. The impact ARG has on the various DCEUS quantification parameters that relate to blood flow is also assessed.

Materials and methods

Patients

Twenty five patients (11 females, 14 males) presenting with colorectal liver metastases were imaged. The overall mean age of the patients was 69 years (range, 47–77), with a male population mean age of 71 years (range, 59–77) and a female population mean age of 67 years (range, 47–72). The patients imaged received a bi-weekly dose of bevacizumab (Avastin; Hoffmann-La Roche, Basel, Switzerland) along with a chemotherapeutic regiment of oxaliplatin (Eloxatin; Sanofi-Aventis, Paris, France) or irinotecan (Camptosar; Pfizer, New York, NY, USA) combined with capecitabine (XELODA; Hoffmann-La Roche, Basel, Switzerland). DCEUS image loops were obtained from each patient for further analysis.

Ethical approval for this study was provided from the institutional review board of our hospital. The nature of the procedure was fully explained to all patients and informed consent was obtained.

Clinical dynamic contrast-enhanced ultrasound (DCEUS) acquisitions

The Philips iU22 scanner (Philips Medical Systems, Bothell, WA, USA) along with the C5-1 curved array probe was utilized for all imaging. System settings were: imaging frequency of 1.7 MHz, power modulation pulsing scheme with a mechanical index (MI) of 0.06, and frame rate between 7 and 10 Hz, depending on the image depth. One-minute loops of lesions were acquired in dual-contrast imaging acquisition mode. A very low-level uniform noise in the image before the arrival of the microbubbles was allowed to ensure that the time-gain-compensation (TGC) was exactly at the threshold of detection. The focus was set a little below the depth of the lesion for a uniform pressure field. A 2.4-mL bolus of microbubble contrast agent Sonovue (Bracco s.p.a., Milan, Italy) was injected via a three-way valve. A constant imaging plane was maintained by the clinician by monitoring the 'tissue' side of the acquisition.

The lesions presented in this study varied in their size, depth, initial vascularity and location. The diameter of the lesions varied between 7.7 and 62.6 mm with a median diameter of 16.8 mm whilst the median depth of the lesions was 5.1 cm with a minimum of 2.55 cm and a maximum of 8.56 cm. Eleven lesions had a hypervascular perfusion pattern, 13 exhibited hypervascular perfusion with hypovascular cores and one lesion displayed hypovascular perfusion with hypervascular ring enhancement on its periphery. One-third of the lesions presented were located in the right lobe of the liver. In addition, seven patients had more than one lesion present in their acquisitions. In these cases the largest lesion was chosen for analysis except for one patient in which the largest lesion was confounded by shadowing artefacts, and so the second largest lesion was chosen.

The patients received no breathing instructions during the DCEUS acquisitions. This was done in order to evaluate the ARG algorithm under various magnitudes of in-plane and out-of-plane respiratory motion induced naturally by the variability in the breathing patterns of the patient population.

Image data analysis

The commercial quantification software QLAB version 8.1 (Philips Medical Systems) was used to analyse the image loops.

A radiologist with over 20 years of experience used both the arterial and late portal phases of the DCEUS loop to accurately draw a ROI around the liver lesion. The specific frame on which the ROI was drawn will be referred to as the "trigger" frame. Time-intensity curves from linearized [16] image data were extracted from QLAB without the use of ARG.

Subsequently, the tissue side loop of each acquisition was imported into MATLAB (2012b, The MathWorks Inc., Natick, MA, USA) in order to implement the ARG algorithm (Fig. 2). Analysis of the image data was performed by a Biomedical Engineering PhD candidate supervised by a professor of bioengineering with more than 20 years of experience in clinical ultrasound research. The frame subtraction technique [17] was utilized to detect the location and intensity of motion throughout the acquisition. Bright moving structures were identified on the trigger frame and the motion intensity corresponding to the position of each structure was recorded. In addition, the content of respiration for the motion associated with each structure was quantified using frequency domain analysis. The structure with the highest degree of respiratory motion was used to construct a ROI on the tissue loop and extract the time-intensity curve. The peaks of the time-intensity curve correspond to the time instances at which the bright moving structure is at the same position as on the trigger frame. Frames that were below 40 % from the peak intensity were rejected as being out of phase with the trigger frame. The threshold value of 40 % was chosen as a good default value preserving enough data points to perform a reliable fit of the lognormal model onto the lesion time-intensity curve and reducing respiratory motion in the DCEUS acquisitions. The intensity data on the lesion time-intensity curve matching the rejected frames were removed. Thus after the implementation of the ARG algorithm the lesion time-intensity curve data were in phase with the trigger frame (Fig. 3a). Details regarding the implementation of the ARG algorithm can be found in the literature [15].

The lognormal indicator dilution model [5] was fitted on to time-intensity curves extracted from lesions with and without the use of ARG. The most common DCEUS quantification parameters [1, 3, 4, 6] are the area under the curve (AUC), the peak intensity (PI), the rise time (RT) and the mean transit time (MTT). The coefficient of determination of the fit of the lognormal model to the data (R^2_{LN}) was also calculated. The R^2_{LN} was used in order to assess whether the ARG procedure improves the quality of the lognormal model fit on to the time-intensity curves, thus improving the reliability of the quantification parameters extracted. The assumption that the quality of the fit of the model to the data improves reliability of DCEUS quantification was suggested in the literature [13, 14].

Another useful parameter that was extracted from the time-intensity curves was the respiration amplitude (RA). RA quantifies how much respiration affects a time-intensity curve and it was calculated using the frequency spectrum of the time-intensity curves extracted with and without the use of ARG. Any significant reduction in the RA with the use of ARG would demonstrate that there is a decrease on the effect of respiration on the lesion time-intensity curve. The RA was calculated based on the fact that the perfusion pattern of the liver lesion changes more slowly compared to components from respiration that vary within a frequency range between 0.1 and 0.5 Hz [18]. The RA was calculated by calculating the area under the frequency spectrum between 0.1 and 0.5 Hz and dividing by the area between 0 to 0.1 Hz (Fig. 3b).

Statistical analysis

For each quantification parameter examined in this study, the distribution before and after ARG was summarized in boxplots indicating the median, first and third quartiles. An outlier was considered as a value that was greater than the third quartile plus 1.5 times the interquartile range (IQR; first – third quartiles) or less than the first quartile minus 1.5 times
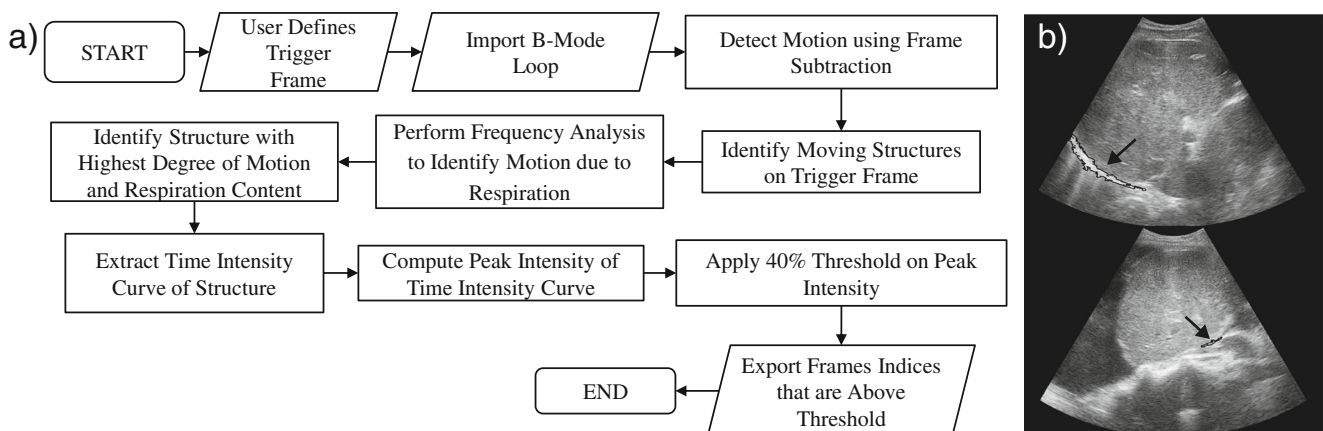
Fig. 2 (a) Flowchart of the procedures used for the implementation of the automatic respiratory gating (ARG) algorithm. (b) Examples of moving structures identified by the ARG algorithm on the trigger frame of the 'tissue' side of the dual contrast imaging acquisition (indicated by the arrows)
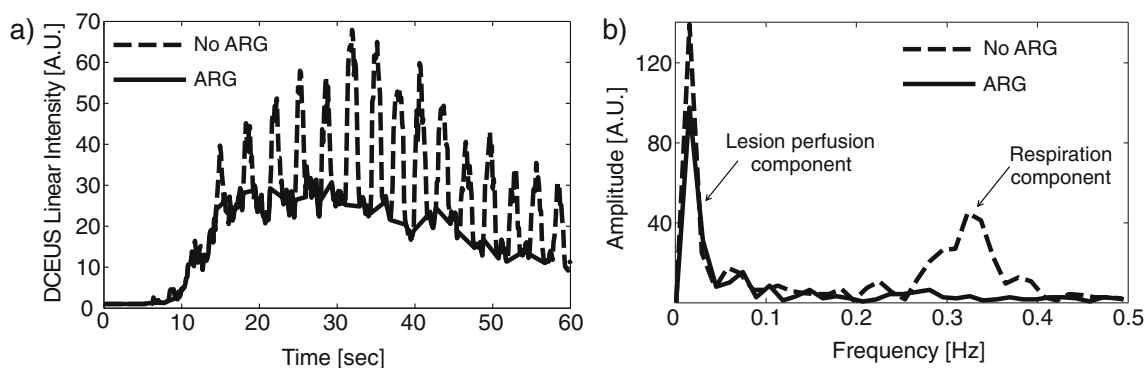
Fig. 3 (a) Example of DCEUS time-intensity curve extracted from a region-of-interest (ROI) encompassing a lesion with and without the use of automatic respiratory gating (ARG). (b) Frequency spectrum of a lesion's time-intensity curve with and without the use of ARG. The slow changing intensity signal originates from the perfusion of the lesion and it lies below 0.1 Hz. The respiratory component lies at 0.1–0.5 Hz. By dividing the area under the curve between the respiration range of 0.1–0.5 Hz over the lesion perfusion range of 0–0.1 Hz the respiration amplitude (RA) was calculated

the IQR. The boxplot bottom whisker was calculated as the minimum value that was not an outlier and the top whisker as the maximum value not considered an outlier.

In order to assess whether ARG has any effect on DCEUS quantification, Wilcoxon signed rank tests were performed between quantification parameters extracted with and without ARG for all the patients participating in the study (N=25). Additionally the Wilcoxon signed rank tests were repeated on quantification parameters extracted from lesion time-intensity curves that had an *RA* of less than 1.5 (N=12). This was done in order to establish the impact of ARG in cases where there was not too much respiration motion present. P-values calculated from the Wilcoxon signed rank test that were less than 0.05 were considered to indicate a significant difference. Statistical analyses were performed using MATLAB's Statistical Toolbox. The power of the Wilcoxon signed rank tests performed was assessed using Monte Carlo simulation. The Monte Carlo simulation was performed in MATLAB and a description of the procedure can be found in the Appendix.

The reduction in the *RA* calculated from lesion time-intensity curves extracted without and with the use of ARG was assessed using a paired t-test. The t-test was chosen because the difference in the distribution of the *RA* data with and without ARG allows for the calculation of power analytically. The significance level for the t-test was set at a p-value of 0.05. The correlation between the quality-of-fit (R^2_{LN}) and the *RA* was assessed using Pearson's *r*.

Results

Relationship between quality of fit and respiration amplitude

Pearson's *r* between the effect of respiration (*RA*) and the quality-of-fit (R^2_{LN}) when ARG was not used had a

value of −0.96 ($P=7.412 \times 10^{-15}$). This strong linear correlation between the *RA* and the quality of fit demonstrated the decline of the accuracy in the modelling of lesion perfusion as the magnitude of respiration increases. When the ARG algorithm was used Pearson's *r* was calculated to be −0.64 ($P=5.449 \times 10^{-4}$). The 33 % decrease in the correlation between *RA* and R^2_{LN} shows the improvement that ARG can have in the modelling of the haemodynamics of liver lesions using DCEUS quantification across the whole range of RA. Furthermore with the use of ARG the R^2_{LN} (the quality of fit of the lognormal model onto the lesion time-intensity curves) was almost constant as *RA* increased. The slope of the linear regression line had a value of −0.11 with the use of ARG compared to −0.31 without ARG. More specifically without the use of ARG 17/25 patients exhibited an R^2_{LN} of less than 0.8; this number decreased to 3/25 patients with the use of ARG (Fig. 4).
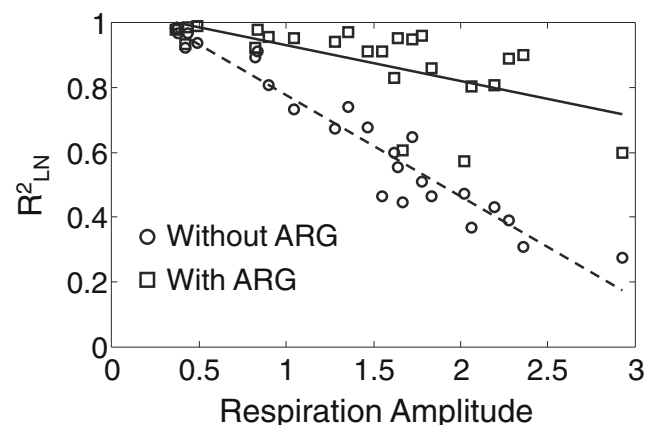
Fig. 4 R^2_{LN} of DCEUS time-intensity curve data fit on lognormal model vs. respiration amplitude with and without the use of automatic respiratory gating (ARG). The linear regression lines of the displayed data are also shown without (dotted) and with (solid) ARG
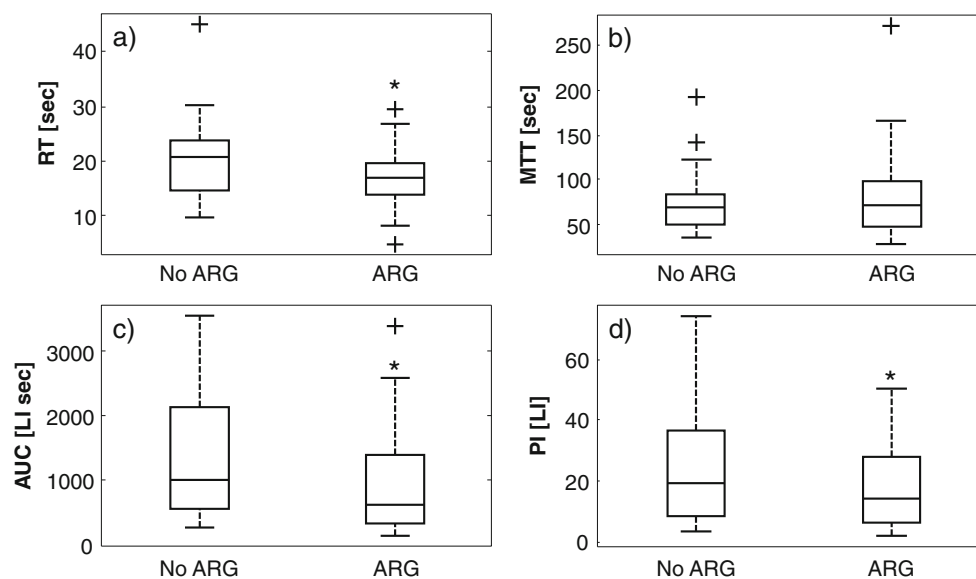
Impact of ARG on quantification parameters

Boxplots of the distribution of DCEUS quantification parameters with and without the use of ARG for the group of all patients (N=25) are presented in Figure 5. Significant differences between RT, AUC and PI with and without the use of ARG were found ($P<0.05$). No significant difference was found between using ARG and not using it for the MTT ($P=0.904$). The power of the Wilcoxon singed rank tests was assessed for each parameter and for a sample size of 25 it was calculated to be 0.75 for the RT (standard deviation 0.03), 0.07 for the MTT (standard deviation 0.01), 0.95 for the AUC (standard deviation 0.01) and 0.87 for the PI (standard deviation 0.02).
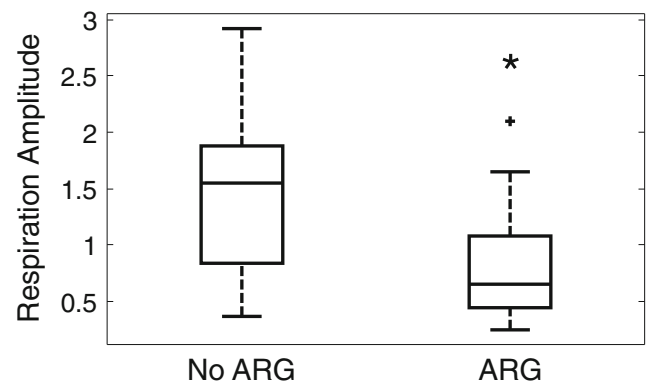
Distribution of the values of the quantification parameters with and without the use of ARG was similar, with the IQR of the boxplots overlapping extensively (Fig. 5). For patients with $RA<1.5$ ARG did not have a significant impact on any quantification parameter ($P>0.077$). This suggests that the use of ARG in cases where there is not too much respiration motion does not affect the quantification data in any way.

Reduction of RA with the use of ARG

The RA calculated from lesion time-intensity curves extracted without the use of ARG was compared to the RA calculated with the use of ARG (Fig. 6). The RA was reduced significantly when ARG was used ($P\leq0.05$).

Fig. 6 Boxplots of the distribution of respiration amplitude (*RA*) with and without the use of automatic respiratory gating (ARG). [+]outliers, *$P\leq$ 0.05, Power>0.9

Discussion

From the results of the statistical analysis on the whole patient population it has been demonstrated that ARG can have a significant impact on the RT, AUC and PI. No statistically significant impact on MTT could be shown. In patients that have an RA of less than 1.5 ARG has no impact on any quantification parameters. Grouls et al. [19] also investigated the effect of respiratory gating on DCEUS quantification parameters using a semi-automatic gating implementation of the manual technique introduced by Averkiou et al. [1]. Grouls et al. [19] showed that gating can have a significant effect on the AUC of bolus injection DCEUS and on the calculation of the retention of targeted microbubbles for molecular ultrasound imaging.

Fig. 5 Boxplots of distributions of (**a**) rise time (RT), (**b**) mean transit time (MTT), (**c**) area under the curve (AUC) and (**d**) peak intensity (PI) quantification parameters with and without the use of automatic respiratory gating (ARG) for all the patients (N=25) participating in the study. *LI* linear intensity. [+]outliers, *$P\leq0.05$

A strong correlation has been demonstrated between R^2_{LN} and RA, with the increase in RA explaining to a large extent the decline in R^2_{LN} of non-ARG processed clinical DCEUS lesion time-intensity curves. This demonstrates that respiration can have a large impact on DCEUS quantification parameters. ARG increases the quality of fit of the time-intensity curve data on to the lognormal model examined in this study across the range of RA values, and thus increases the accuracy of the extracted quantification parameters.

The mean increase in R^2_{LN} across the patient population expressed as a percentage is 37. In the literature 15 % and 11 % increases in the quality of fit were reported by Rognin et al. [13] in the application of motion correction on the parametric imaging of DCEUS of the kidney and liver, respectively. A mean increase between the quality of fit factor before and after motion correction of 15 % was reported by Zhang et al. [14] for the parametric imaging of ten liver DCEUS loops. The above two studies [13, 14] involve the technique of parametric imaging and report the quality of fit on a pixel-to-pixel basis. The presence of noise on data sampled from single pixels or groups of pixels is expected to be greater than those of the present work. Thus any comparison of the results of the mentioned studies with the current study needs to take into account the detrimental effect that the increased noise will have on the quality of fit reported. Furthermore, these studies did not quantify the presence of respiration in their data thus making any comparisons with the current study even more complicated.

In addition to the increase in R^2_{LN} with the use of ARG, the RA was also decreased significantly in time-intensity curves of lesions. This reduction in the RA with the use of ARG further demonstrates the effectiveness of the ARG algorithm in removing respiratory motion from lesion time-intensity curves and increasing the accuracy of DCEUS quantification. By increasing the accuracy of in-vivo DCEUS quantification parameters the clinician can perform a more accurate diagnosis, e.g. on the response of the patient to treatment. Accurate tumour microflow measurements may lead to a decision to be made in regards to continuing with the current treatment or altering the treatment, which can result in a better clinical outcome or a reduction in expenditure on ineffective treatments.

Although this study evaluates the use of ARG on DCEUS quantification, qualitative evaluation of image loops [20] may also benefit from such a motion-correction technique. By applying ARG on image loops during review, the removal of out-of-plane motion results in a more accurate depiction of the area. For example, small lesion vessels stay in-plane and show their feeding patterns.

Other post-processing procedures for treating respiratory motion on DCEUS loops of liver lesions can be found in the literature. One technique proposed by Averkiou et al. [1] is for the clinician to manually reject frames in which the diaphragm position deviates from a reference location. This technique does not require any special precautions to be taken during the DCEUS acquisition but it is time consuming and operator dependent. The present ARG algorithm works by detecting bright structures moving with a frequency within the range of respiration (0.1–0.5Hz). Often such a bright structure is the diaphragm but others may be encountered also. In 17/25 cases analysed the diaphragm was automatically detected. In the rest other bright image structures were detected (Fig. 2b).

Studies on methods for automatic respiratory motion correction have been published in the literature [11–14, 21]. A technique based on independent component analysis (ICA) was introduced by Renault et al. [12] where the respiratory kinetics curve could be manually extracted from the components derived from the ICA. Frames of the loop that were part of the end phases of the respiratory cycle could be isolated by using a threshold on the respiratory kinetics curve. Furthermore, Mule et al. [11] developed a fully automatic algorithm that utilizes principal component analysis (PCA) to perform respiratory gating and extract frames that belong to the end phases of the respiratory cycle. Although the ICA and PCA algorithms proposed can correct for both in-plane and out-of-plane respiratory motion, they are limited in extracting only the end phases of the respiratory cycle. It is possible that part of the lesion, or even the whole lesion, could be absent on the imaging plane during the end-respiratory phases.

Image registration has also been used in the literature to correct for respiratory motion. Zhang et al. [14] used a 2D image registration technique with frame selection in order to remove both in-plane and out-of-plane motion but a computational time of 3 min per 100 frames could limit the use of the algorithm in the clinic. Rognin et al. [13, 21] used a 2D rigid registration technique with translation and rotation to register frames with a reference frame; however, this technique lacked a scheme for removing out-of-plane respiratory motion. Both the image registration algorithms discussed required the user to draw ROI(s) on frames to define the area on the image into which the registration process would take place.

The ARG algorithm clinically evaluated in the present study is fully automated requiring the user to only provide a reference frame; it is fast since it can process 100 frames in less than a second, it allows for the extraction of any breathing cycle phase required by the operator, and it removes both in-plane and out-of-plane respiratory motion [15, 22].

A limitation of the present work is the use of a fixed gating threshold for all of the patients. The gating threshold regulates what percentage of frames that are out of synchronization with the trigger frame are allowed to be part of the ARG processed loop. By setting the gating threshold too high a large number of frames that are out of phase with the trigger are quantified leading to uncertainty in the results. If the gating threshold is low it includes a very small number of frames to be quantified and possibly too few to be able to perform a robust fit of the model. Since the breathing patterns of patients can differ significantly, the clinician performing the quantification analysis can easily

adjust the threshold for each patient during quantification of the loops. A 40 % threshold was used on all patients to standardize the procedure as was previously reported in the literature [15].

Moreover it is possible to manually reject frames of the ARG processed loop to further improve the quantification analysis. This option was not used in this study in order to ensure reproducibility and objectivity. Some quantification software offer the ability to perform motion compensation based on image registration algorithms. Since this work focused on evaluating a specific ARG technique, no further motion compensation was performed on the extracted data. In clinical practice, conventional motion compensation algorithms may be applied to ARG processed loops and further improve the quantification accuracy.

In conclusion, the ARG algorithm examined had a strong impact on clinical DCEUS quantification parameters. Furthermore, the use of ARG resulted in an overall increase in the quality of fit of the lognormal model and a significant decrease in the respiration amplitude. This study demonstrates the implications that respiration can have on liver DCEUS; the same technique may also be applied to study the impact of respiration on DCEUS when studying the perfusion of other organs, but further validation studies are necessary.

Appendix: Calculation of the power of the Wilcoxon signed rank tests

Some assumptions must be made in order to calculate the power of the Wilcoxon signed rank tests performed in this study. The first assumption was that the parameters from before and after the application of ARG were part of the same distribution. Two-sample Kolmogorov-Smirnov tests were performed on the quantification parameters before and after the application of ARG demonstrating that the parameters were part of the same distribution ($P > 0.05$). The Monte Carlo simulation made use of this by concatenating the before and after ARG parameters into one population from which the mean and standard deviation were calculated.

Another assumption made in order to calculate the power was that the concatenated distributions of the quantification parameters along with the differences between the parameters before and after the application of ARG were normal. This was demonstrated using one-sample Kolmogorov-Smirnov tests at a significance level of 0.05. This assumption was used

in the Monte Carlo simulation in order to simulate random samples from normal distributions.

The Monte Carlo simulation for a particular pair of quantification parameters extracted without ARG (A) and with ARG (B) is described in the following steps:

Step 1   Calculate mean (μ_{noARG}) and standard deviation (σ_{noARG}) of the concatenated vector of A and B.

Step 2   Calculate mean (μ_{diff}) and standard deviation (σ_{diff}) of the differences (A minus B).

Step 3   Set the sample size equal to 25 (n=25).

Step 4   Simulate quantification parameters extracted without ARG by randomly sampling 25 data points (n=25) from a normal distribution with a mean equal to μ_{noARG} and a standard deviation equal to σ_{noARG}.

Step 5   Simulate differences between quantification parameters extracted with and without ARG by randomly sampling (n=25) from a normal distribution with a mean equal to μ_{diff} and a standard deviation equal to σ_{diff}.

Step 6   Simulate quantification parameters extracted with ARG by subtracting the random sample of step 4 from that of step 5.

Step 7   Perform a Wilcoxon signed rank test between the simulated parameters extracted with and without the use of ARG at a significance level of 0.05.

Step 8   Increment counter variable (CV) by one if the test returns a significant difference between the simulated parameters extracted with and without the use of ARG.

Step 9   Repeat steps 4–8 200 times.

Step 10   Calculate the power by dividing CV over 200.

Step 11   Repeat steps 4–10 20 times to calculate the uncertainty of the power calculation.

References

1. Averkiou M, Lampaskis M, Kyriakopoulou K et al (2010) Quantification of tumor microvascularity with respiratory gated contrast enhanced ultrasound for monitoring therapy. Ultrasound Med Biol 36:68–77

2. Bertolotto M, Pozzato G, Crocè LS et al (2006) Blood flow changes in hepatocellular carcinoma after the administration of thalidomide assessed by reperfusion kinetics during microbubble infusion: preliminary results. Invest Radiol 41:15–21

3. Lassau N, Koscielny S, Chami L et al (2011) Advanced hepatocellular carcinoma: early evaluation of response to bevacizumab therapy at dynamic contrast-enhanced US with quantification–preliminary results. Radiology 258:291–300

4. Lassau N, Koscielny S, Albiges L et al (2010) Metastatic renal cell carcinoma treated with sunitinib: early evaluation of treatment response using dynamic contrast-enhanced ultrasonography. Clin Cancer Res 16:1216–1225

5. Strouthos C, Lampaskis M, Sboros V et al (2010) Indicator dilution models for the quantification of microvascular blood flow with bolus administration of ultrasound contrast agents. IEEE Trans Ultrason Ferroelectr Freq Control 57:1296–1310

6. Dietrich CF, Averkiou MA, Correas J-M et al (2012) An EFSUMB introduction into Dynamic Contrast-Enhanced Ultrasound (DCE-US) for quantification of tumour perfusion. Ultraschall Med 33: 344–351

7. Leen E, Averkiou M, Arditi M et al (2012) Dynamic contrast enhanced ultrasound assessment of the vascular effects of novel therapeutics in early stage trials. Eur Radiol 22:1442–1450

8. Tang M-X, Mulvana H, Gauthier T et al (2011) Quantitative contrast-enhanced ultrasound imaging: a review of sources of variability. Interface Focus 1:520–539

9. Lampaskis M, Averkiou M (2010) Investigation of the relationship of nonlinear backscattered ultrasound intensity with microbubble concentration at low MI. Ultrasound Med Biol 36:306–312

10. Thapar A, Shalhoub J, Averkiou M et al (2012) Dose-dependent artifact in the far wall of the carotid artery at dynamic contrast-enhanced US. Radiology 262:672–679

11. Mulé S, Kachenoura N, Lucidarme O et al (2011) An automatic respiratory gating method for the improvement of microcirculation evaluation: application to contrast-enhanced ultrasound studies of focal liver lesions. Phys Med Biol 56:5153–5165

12. Renault G, Tranquart F, Perlbarg V et al (2005) A posteriori respiratory gating in contrast ultrasound for assessment of hepatic perfusion. Phys Med Biol 50:4465–4480

13. Rognin N, Campos R, Thiran J, et al (2006) A new approach for automatic motion compensation for improved estimation of perfusion quantification parameters in ultrasound imaging. Proc. 8th French Conf. Acoust. Tours, France, pp 61–65

14. Zhang J, Ding M, Meng F et al (2011) Respiratory motion correction in free-breathing ultrasound image sequence for quantification of hepatic perfusion. Med Phys 38:4737–4748

15. Christofides D, Leen E, Averkiou M (2014) Automatic respiratory gating for contrast ultrasound evaluation of liver lesions. IEEE Trans Ultrason Ferroelectr Freq Control 61:25–32

16. Gauthier TP, Averkiou MA, Leen ELS (2011) Perfusion quantification using dynamic contrast-enhanced ultrasound: the impact of dynamic range and gain on time-intensity curves. Ultrasonics 51: 102–106

17. Jain A (1989) Fundamentals of Digital Image Processing.1st edn. Prentice-Hall, Englewood Cliffs, p 400

18. Fleming S, Thompson M, Stevens R et al (2011) Normal ranges of heart rate and respiratory rate in children from birth to 18 years of age: a systematic review of observational studies. Lancet 377:1011–1018

19. Grouls C, Hatting M, Tardy I et al (2012) Development and validation of an intrinsic landmark-based gating protocol applicable for functional and molecular ultrasound imaging. Eur Radiol 22:1789–1796

20. Roche V, Pigneur F, Tselikas L et al (2015) Differentiation of focal nodular hyperplasia from hepatocellular adenomas with low-mechanical-index contrast-enhanced sonography (CEUS): effect of size on diagnostic confidence. Eur Radiol 25:186–195

21. Rognin NG, Arditi M, Mercier L et al (2010) Parametric imaging for characterizing focal liver lesions in contrast-enhanced ultrasound. IEEE Trans Ultrason Ferroelectr Freq Control 57:2503–2511

22. Christofides D, Leen E, Averkiou M (2014) Improvement of accuracy of liver lesion DCEUS quantification using automatic respiratory gating. 19th Eur. Symp. Ultrasound Contrast Imaging. pp 69–73